CrossMark

ORIGINAL PAPER

Molecular and morphological characterization of poly(L-lactic acid-co-glycolic acid) P(L-LA/GA) copolymers prepared by Azeotropic distillation

Mariana Gutiérrez-Sánchez[1] · **Francisco Javier Medellín-Rodríguez**[1] · **Laura Ivone Silva-de- la- Cruz**[1]

Abstract The synthesis and molecular/morphological characterization of poly(L-lactic acid-co-glycolic acid) P(L-LA/GA) copolymers were investigated. The optimum reaction conditions were first determined by azeotropic distillation polymerization of poly(L-lactic acid) P(L-LA) homopolymers. Once the best reaction conditions were determined, the P(L-LA/GA) copolymers were synthesized by increasing the glycolic acid (GA) proportion in the reaction mixture from 0 to 7.5 mol%. The ^{13}C NMR technique allowed inferring the formation of a copolymer with increasing segmental GA characteristics. These last with the potential to be rejected from the main crystals, assumption that was supported by the convergence of the crystallization and melting temperatures as the molar ratio of GA increased. The diffraction patterns of the copolymers demonstrated the gradual formation of α-α" crystal blends with the GA content and the crystallization and meting results allowed conclude that the increasing number of GA units in the main chain was related to molecular rejection, which resulted in a secondary exclusion phase, the major contribution to melting at the first melting endotherm. This behavior was in correlation with the step-like crystallization and melting mechanism previously proposed for high temperature engineering polymers.

Keywords P(L-LA/GA) copolymers · Morphology/property relationships of polymers

✉ Francisco Javier Medellín-Rodríguez
francmr@uaslp.mx

1   Facultad de Ciencias Químicas, Universidad Autónoma de San Luis Potosí, Av. Dr. Manuel Nava 6, Zona Universitaria, 78216 San Luis Potosí, S.L.P, Mexico

Introduction

Aliphatic polyesters that are derived from lactic acid (LA) and glycolic acid (GA) exhibit the potential for biomedical applications due to their biodegradable and biocompatible properties [1–5]. Poly(lactic acid) (PLA) can be obtained in three isomeric forms (i.e., dextrorotatory (D), levorotatory (L) and racemic (D-L)). Therefore, depending on the L and D content, a number of different stereochemical structures are formed, ranging from amorphous to semicrystalline polymeric structures with different morphological characteristics. The isomeric PLA forms exhibit a range of characteristic temperatures. For example, the P(L-LA) glass transition temperature (Tg) is reported between 50 and 80 °C and the melting temperature (Tm) between 130 and 180 °C [6, 7]. It is important to note that the L form is ideal from a toxicological point of view because it is easily metabolized by the human body [8, 9]. Poly(glycolic acid) (PGA) is a linear, rigid, aliphatic polyester with a high crystallinity content (45–55 %) and melting points and glass transitions between 220 and 225 °C and 30–40 °C, respectively. PGA can also be naturally metabolized by the human body. However, the high crystallinity of this polymer limits its solubility to highly fluorinated organic solvents, such as hexafluoride isopropanol [10].

As previously mentioned, biocompatibility and biodegradability are two attractive properties for biomedical applications. Therefore, the generation of both properties in a single polymeric product has recently become a primary focus in the field of polymer science. This hypothetic polymer can be prepared by polymerizing L-lactic acid (L-LA) and glycolic acid (GA). Therefore, in the present study, the corresponding monomers were copolymerized via azeotropic distillation using several molar ratios of the two reactants. This type of polymerization has at least two advantages on traditional

polycondensation, it renders higher molecular weights and water removal is easier [11].

The main objective of this study was to synthesize a range of copolymer products to determine their molecular characteristics and morphological properties in order to gain insight into their behavior. In particular, the conceptual extension to biopolymers of the step-like crystallization and melting mechanism, previously reported in high temperature polymers.

Experimental

Materials

Most of the chemical agents were obtained from Sigma-Aldrich Inc. including L-lactic acid (L-LA, 85 wt% aqueous solution), glycolic acid (GA), tin (II) chloride dihydrate (SnCl$_2$.2H$_2$O), p-toluenesulfonic acid (CH$_3$C$_6$H$_4$SO$_3$H), tin powder (Sn) and molecular sieve (3 Å) beads. Xylene (C$_6$H$_4$(CH$_3$)$_2$) was obtained from Analytyka, chloroform (CCl$_4$) was obtained from Caledon, and methanol (CH$_3$OH) was obtained from Julmek Inc.

Copolymer synthesis

The optimization of reaction conditions forming P(L-LA) was made through the same synthesis method, therefore, in this section only the copolymerization process is described. The copolymerization reaction was carried out using azeotropic distillation according to the method reported by Ajioka et al. [12]. For this purpose, the distillation process was done in two steps using several molar ratios of L-lactic acid (L-LA) and glycolic acid (GA). The first step involved the formation of oligomers and the complete removal of residual water, which was performed in a batch reactor equipped with a water separator Dean Stark arm and a temperature controller. In this step, 20 g of L-LA and GA with 0.4 wt% (SnCl$_2$.2H$_2$O/TSA molar ratio 1:1) along with 200 ml of p-xylene were mixed and heated to the boiling point of p-xylene (i.e., 138 °C). A portion of the p-xylene and extracted water was collected in the separator arm, where water and p- xylene formed two phases. In this form, p-xylene was recycled to the reaction zone by decantation. This process required a total reaction time of 2 h. The second step (increase of the molecular weight) was also performed using azeotropic distillation at 138 °C. In this case, the reactor was a Soxhlet extractor packed with molecular sieve beads. Both the oligomer and fresh solvent (p-xylene) were placed into the reactor, and the distillation process proceeded for 48 h until the resulting mixture became concentrated. The reaction product was dissolved in chloroform and subsequently precipitated with methanol. This solid was ultimately filtered and dried at room temperature for 48 h.

Characterization techniques

The thermal properties were determined using a Perkin Elmer DSC-7 differential scanning calorimeter. In this case, 5 ± 0.1 mg samples were placed into sealed aluminum sample holders. All of the thermal scans were performed at 10 °C/min. To scan the amorphous state, the corresponding samples were subjected to heating from room temperature up to 210 °C, where they were maintained for 3 min to erase the original thermal history. Then, a quenching process was quickly carried out to 25 °C at a nominal rate of 500 °C/min followed by linear heating at 10 °C/min up to 210 °C. From the thermal traces, the glass transition (Tg), crystallization (Tc) and melting temperatures (Tm) were obtained. For the isothermal crystallization experiments, cooling from the melt was quickly performed to the isothermal crystallization temperature (Tc), where the sample remained for 30 min prior linear heating at 10 °C/min to 210 °C. The molecular weight of the synthesized samples was measured in a Waters Alliance 2695 gel permeation chromatograph (GPC), coupled to an ultraviolet detector Waters 2998 (wavelength 248 nm). Chloroform was used as solvent and mobile phase at a flow rate of 1.0 mL/min at 30 °C. The calibration curve was obtained using the standard polystyrene samples. For the circular dichroism (CD) studies, the polymeric reaction products were dissolved in chloroform at a concentration of 1 g/DL, and the resulting dilutions were characterized by CD on a Jasco spectropolarizer J-810, which used a 450 W Xenon lamp as the power source. The molecular characteristics of the products were determined by nuclear magnetic resonance (NMR), and the ^{13}C NMR and ^{1}H NMR spectra were obtained using a Brokers Advance spectrophotometer at 500 MHz. To obtain the spectra, the polymeric samples were dissolved in deuterated chloroform using tetramethylsilane as an internal standard. The ^{1}H NMR and ^{13}C NMR spectra were obtained using an acquisition time of 32 s and 128 s, respectively. The chemical identification of the products was performed using Fourier transform infrared spectroscopy (FTIR) on a Bruker Tensor 27 spectrophotometer. The corresponding samples were examined through attenuated reflection (ATR) using a resolution of 4 cm^{-1} and 32 scans per sample. Wide angle X-ray diffraction (WAXD) patterns were obtained on a PANalytical X'Pert Pro instrument using Cu-Kα radiation with a wavelength of 1.54 Å, an accelerating voltage of 35 kV and a filament current intensity of 30 mA within a 2θ scanning range of 2 to 30°. For the polarized optical microscopy (POM) experiments, two Mettler FP82HT hot-stages were used and the quick transfer method was applied. In this case, samples were first melted for 3 min at 180 °C and then they were quickly transferred to the isothermal crystallization hot-stage where they remained for 30 min. After this period of time, linear heating at 10 °C/min was applied and micrographs were taken at different temperatures.

Fig. 1 DSC heating traces from the amorphous state of P(L-LA) based on the reaction time: **a** Std. 2000 g/g-mol, **b** 24 h, **c** 48 h and **d** 72 h
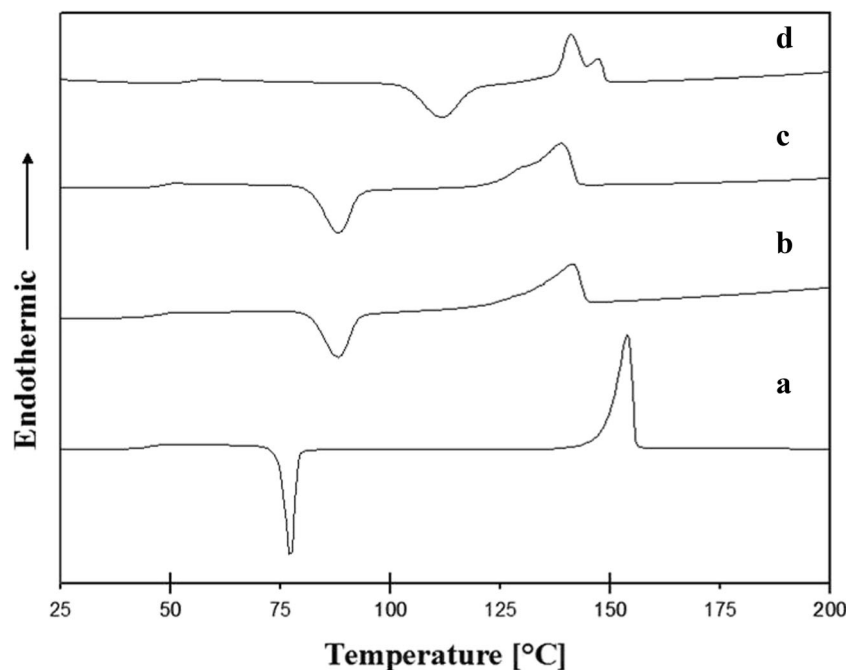
Results and discussion

Optimization of reaction conditions with P(L-LA)

The analysis of the structural and thermal properties of the P(L-LA) products, taking into consideration the main variables of the reaction system, confirmed the formation of P(L-LA). From these studies, an optimum synthesis route was determined to prepare the desired P(L-LA/GA) copolymers. The systematically studied variables and their main characteristics are discussed in the following sections.

Reaction time

Figure 1 shows the thermal traces, which involve heating from the amorphous state, of P(L-LA) after polymerization for 24–72 h. In this case, 0.4 wt% of a Sn catalyst was used, and the low molecular weight P(L-LA) (2000 g/g-mol) was employed as the reference. In the first part of the thermal trace, there are two main characteristics; the glass transition temperature and the exothermic peak (between 80 and 120 °C) associated with the overall non-isothermal crystallization from the glassy state. In contrast, some more complex characteristics are involved during the melting process, where up to two melting endotherms are observed. Table 1 quantitatively shows that both T_g and T_c directly depend on the reaction time, which indicates that the increasing molecular weight also increases molecular entanglements and as a consequence T_g. In contrast to the single melting behavior of the standard, a complex evolution was observed of the different products in the melting zone. After 24 h of reaction (Fig. 1b), an additional endotherm (I) was observed, which gradually transforms into a new pronounced endotherm at long reaction times. Although in much lower proportion, a similar evolution resulted from an increase in the molecular weight of engineering polymers, such as PET, and was explained in terms of the increase in thin secondary crystals that melt at lower temperatures [13], topic that will be discussed later.

Table 1 Molecular weight, characteristic temperatures and enthalpies of P(L-LA) as a function of the polymerization time

Time (h)	Mn [b] (Da)	Mw [b] (Da)	Mw/Mn [b]	T_g (°C)	T_c (°C)	ΔH_c (J g^{-1})	ΔH_m (J g^{-1})	χ_m (%)
NA	NA	NA	NA	45.5	77.2	-35.4	59.7	63.7[a]
24	2362	3410	1.44	47.2	87.9	-36.2	35.2	37.6
48	3320	4980	1.50	47.7	88.0	-35.3	48.1	51.3
72	10,872	39,687	3.65	54.4	111.5	-34.3	35.9	38.3

NA Not applicable

[a] Reference standard

[b] GPC determined

Fig. 2 DSC thermal traces after heating the amorphous state of the P(L-LA) reaction products after 48 h. of polymerization using: **a** Sn and **b** SnCl$_2$.2H$_2$O/TSA 1:1
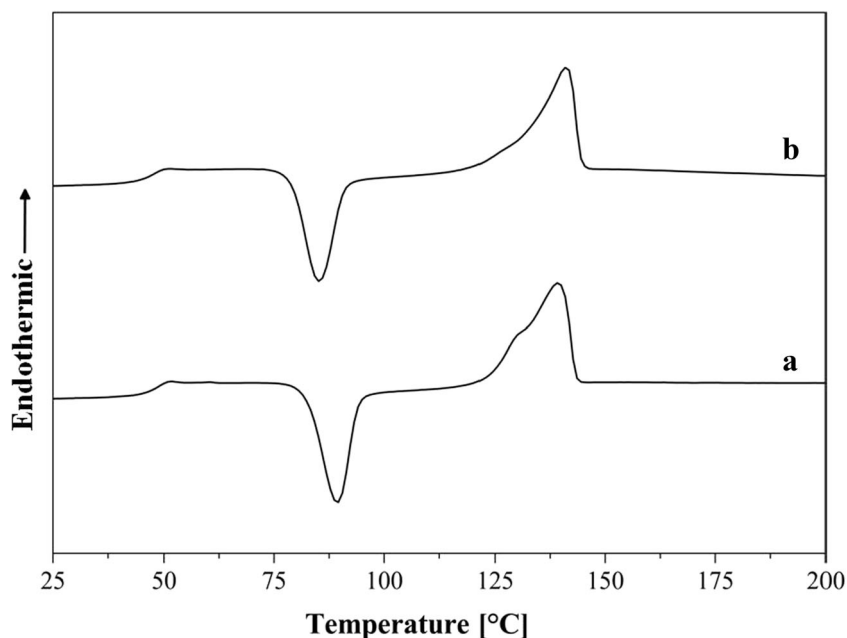

The total crystalline content (χ_m) shown in Table 1 was calculated from the DSC data using the following equation [11]:

$$\chi_m\% = 100 \frac{(\Delta H_m)}{\Delta H_m^0} \tag{1}$$

where ΔH_m is the total enthalpy of melting and ΔH^0_m (93.6 J/g) is the melting enthalpy of the P(L-LA) crystals with infinite crystal thickness [11]. However, the nature of the quenching experiment does not allow for the determination of the

crystallinity from the DSC heating curve, without involving secondary effects such as recrystallization. Therefore, we consider the increase in Tg with reaction time (see Table 1) and the inverse relationship between time and the crystallization enthalpy of the sample (area under the crystallization curve), as an indication of the formation of higher molecular weights as the reaction time increased. This is because macromolecules with higher molecular weights have a higher degree of entanglement, which impedes the molecular flux toward crystallization. The crystallization χ_m values do not have a particular meaning due to the morphological change in the system
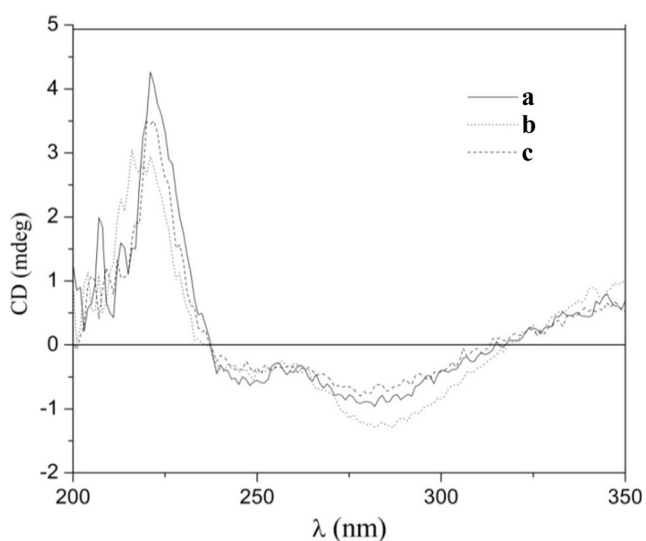
Fig. 3 Circular dichroism (CD) of P(L-LA) depending on the type of catalyst: **a** P(L-LA) standard; **b** polymerized product with SnCl$_2$.2H$_2$O/TSA (1:1); **c** product using Sn
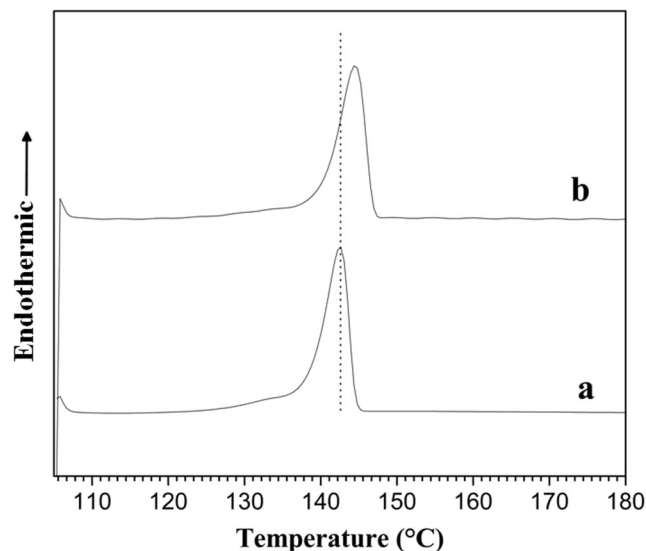
Fig. 4 DSC Heating traces after isothermal crystallization at 105 °C for 30 min: **a** polymerization with Sn (48 h) and **b** polymerization with SnCl$_2$.2H$_2$O/TSA (48 h)

Table 2 GPC molecular weights as a function of the type of catalyst

Type of catalyst	Mn [a] (Da)	Mw [a] (Da)	Mw/Mn
Sn	3474	4759	1.37
SnCl$_2$.2H$_2$O/TSA	3320	4980	1.50

[a] GPC determined

during heating. The correlation between reaction time and thermal behavior was also corroborated with the molecular weight and polydispersity degree which were GPC determined. The results in Table 1 show that the molecular weight increases with reaction time at approximately constant polydispersity degree. Higher reaction times maintain the increase of molecular weight although the width of the distribution tends to widen.

Catalyst effect

Two catalysts [2, 12] were employed in this study including a SnCl$_2$.2H$_2$O/TSA mixture in a 1:1 M ratio and Sn powder. These catalysts were used for azeotropic polymerization of the L-lactic acid monomer at a concentration of 85 wt%. In both cases, the reaction products were thermally scanned, and the results after quenching the melt for 48 h are shown in Fig. 2.

The results in Fig. 2 demonstrate slight differences in the crystallization and melting curves. For example, using SnCl$_2$.2H$_2$O/TSA (Fig. 2b) good definition in the melting curve is observed along with a 5 °C decrease in the crystallization temperature and a 2 °C increase in the melting temperature. For the Sn catalyst (Fig. 2a), an overlapped melting endotherm was observed at 128 °C, indicating melting of two crystalline phases. This was an indication that the type of catalyst motivates changes in crystal morphology, particularly when Sn is used as the catalyst. This morphological change occurs during crystallization and

shows off during melting, as will be again discussed in the next section.

Molecular order

Considering the differences in the thermal traces shown in Fig. 2, where the effect of the catalyst is compared, a complementary evaluation of the two reaction products was performed. For this purpose, the stereochemical structure of the polymeric products was evaluated in terms of circular dichroism (CD) using again the P(L-LA) standard as a reference.

The results in Fig. 3 show a positive peak at 220 nm in the far UV region for all of the samples. This positive peak has been associated with a helical structure assigned to the $\pi \rightarrow \pi^*$ electronic transition of the ester group [14, 15]. The CD signal, that passes through an optically active sample, is the result of the difference between the absorption of the circularly polarized light to the left (D) and right (L) directions of the polarizer. The P(L-LA) exhibited a positive peak, and the reaction products were compared to this standard. The amount of L stereoisomer depended on the absorption intensity. The Sn catalyzed system exhibited the lowest intensity. Therefore, the P(L-LA) product obtained using the SnCl$_2$.2H$_2$O/TSA catalyst had a higher L stereoisomer (i.e., higher structural order along the polymeric chain).

The heating traces of the two polymeric systems are shown in Fig. 4, after isothermal crystallization at 105 °C for 30 min using the SnCl$_2$.2H$_2$O/TSA and Sn catalysts. An increase of 2 °C in the melting endotherm of the SnCl$_2$.2H$_2$O/TSA polymerized product was observed (Fig. 4b), which denotes the formation of more perfect crystals. This result is due to the higher structural order that requires a higher temperature for melting.

The samples corresponding molecular weights are shown in Table 2, where the close similarity of molecular weights in both cases gives support to the proposition that the catalyst mostly influences the nature of the polymerized product.
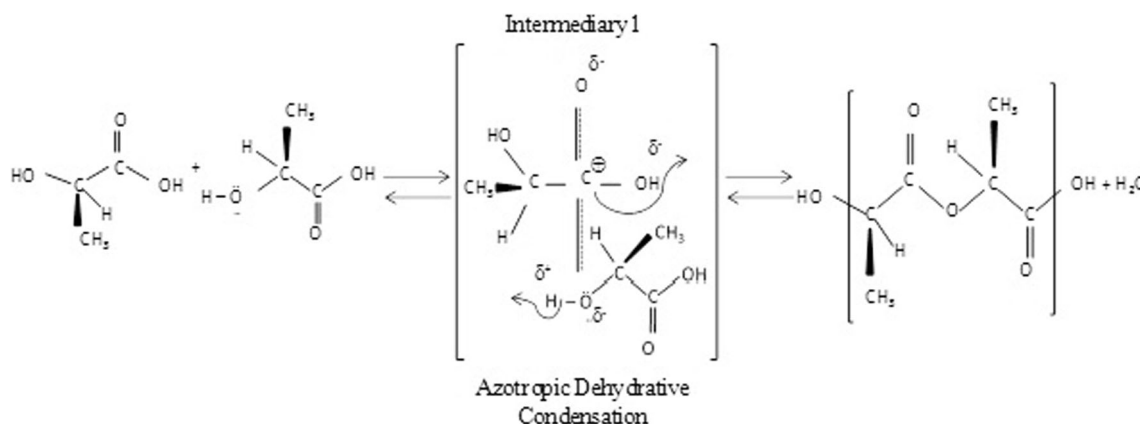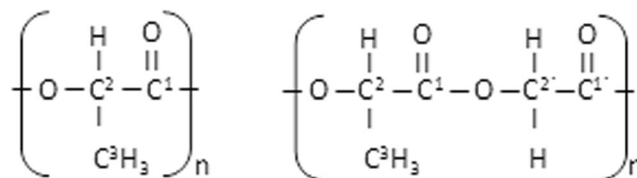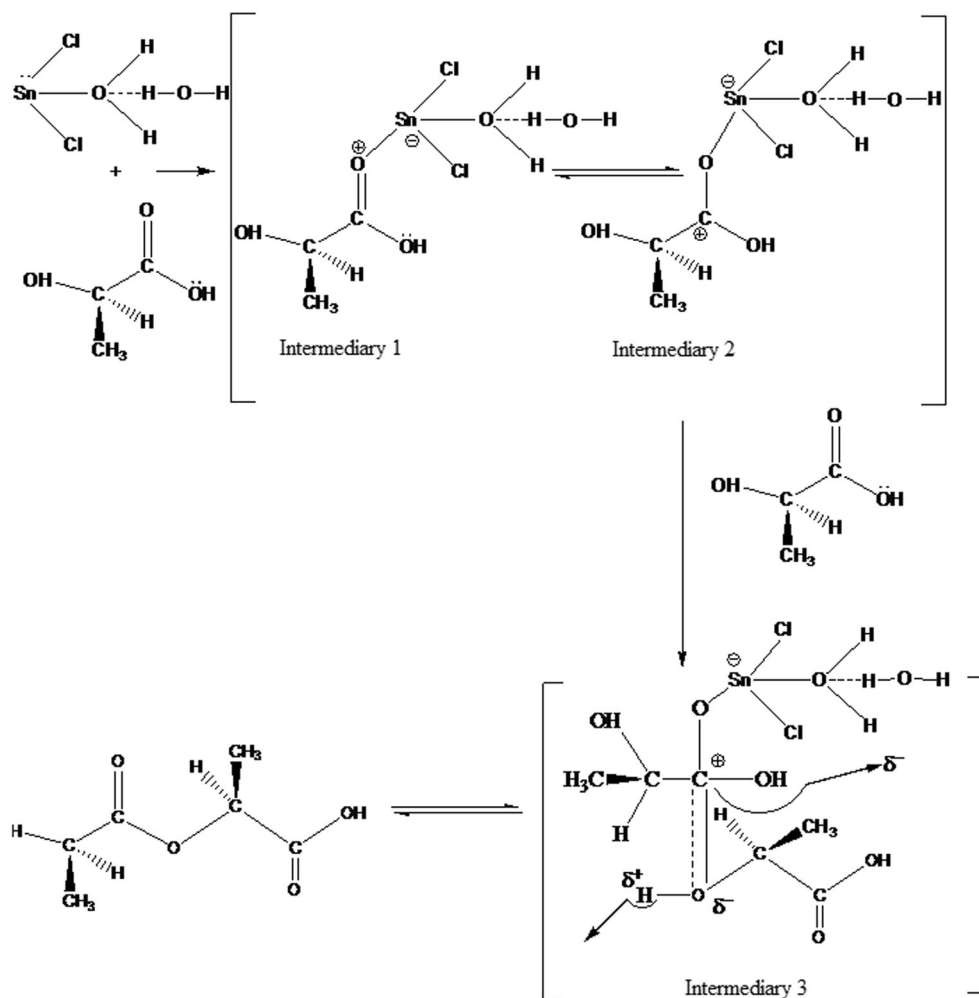

Fig. 5 Adaptation of the reaction mechanism for P(L-LA) polymerization via an uncatalyzed reaction

The simple mechanism of ester formation proceeds through the generation of an intermediate [16], as shown in Fig. 5. This intermediate is produced through nucleophilic attack by one of the electron pairs on the alcohol oxygen. This attack can be perpendicular to the carbon atom of the carbonyl group forming a carbocation. Then, the proton migrates to the hydroxyl group of the acid, which is expelled from the intermediate as OH⁻ and reacts with the H⁺ of the alcohol.

To accelerate the formation of the intermediate species, a catalyst is required. A simple tentative reaction mechanism using the $SnCl_2.2H_2O$/TSA catalyst is shown in Fig. 6. Here, the catalyst forms a coordinated link with the oxygen in the acid group, and then, a positive charge is generated on the carbon atom of the carbonyl group, which is subsequently attacked by the nucleophile.

The formation of complex intermediates with both catalysts follows the same chemical route. However, more bulky intermediates will be formed with $SnCl_2.2H_2O$/TSA, which could prevent the nucleophilic attack, decreasing the formation of stereoisomers.

Fig. 7 Labeling of the atoms in P(L-LA) and P(L-LA/GA)

Copolymers

Once the optimum polymerization conditions were determined, the copolymerization of lactic acid and glycolic acid was achieved using the same synthesis route. However, the chemical, thermal and morphological evolution of the products was studied now as a function of the molar ratio of glycolic acid (GA) in the reaction mixture.

Configuration and molecular weights

¹H NMR spectroscopy was used to calculate the molar composition of the copolymers using equations (2) and (3) and the atomic positions specified in Fig. 7.

Fig. 6 Simple proposed polymerization mechanism for P(L-LA) using $SnCl_2.2H_2O$/TSA as catalyst

Table 3 Theoretical and experimental values of the copolymers molar ratio from ^{1}H NMR

Theoretical lactic/glycolic (mole % L-LA)/ (mole % GA)	Mn [a] (Da)	Mw [a] (Da)	Mw/Mn [a]	Experimental lactic (mole %) [b]	Experimental glycolic (mole %) [b]
100.0/0.0	3320	4980	1.50	100.0	0.0
97.5/2.5	3691	5872	1.59	96.6	3.4
95.0/5.0	6041	10,396	1.72	94.1	5.9
92.5/7.5	NA	NA	NA	90.7	9.3

NA Not applicable

[a] GPC determined

[b] NMR determined

$$\%\text{Lactic} = \frac{(H^3)\text{Integral of the area}/3}{(H^3)\text{Integral of the area}/3 + (H^{2'})\text{Integral of the area}/2} \times 100 \quad (2)$$

$$\%\text{Glycolic} = \frac{(H^{2'})\text{Integral of the area}/2}{(H^3)\text{Integral of the area}/3 + (H^{2'})\text{Integral of the area}/2} \times 100 \quad (3)$$

The methyl proton signal for the lactic acid group (H^3) appears as a doublet between 1.49–1.69 ppm, and the signal for the methylene group in glycolic acid ($H^{2'}$) appears between 4.60–4.90 ppm [17, 18].

A summary of the theoretical and experimental values for the molar composition determination is shown in Table 3,

where higher experimental values are observed for the glycolic acid content with respect to the initial monomer feed composition. However, these differences are associated to the reactivity of the glycolic acid monomer, which is higher than the reactivity of the lactic acid monomer [17]. The corresponding molecular weights, GPC determined, are also included in Table 3, where an augment in molecular weight is observed for the low GA compositions at relatively constant polydispersity. We have reported that the molecular weight affects the first melting endotherm in several polymers [13, 19] through molecular rejection. In the present case the increase in the number average molecular weight is
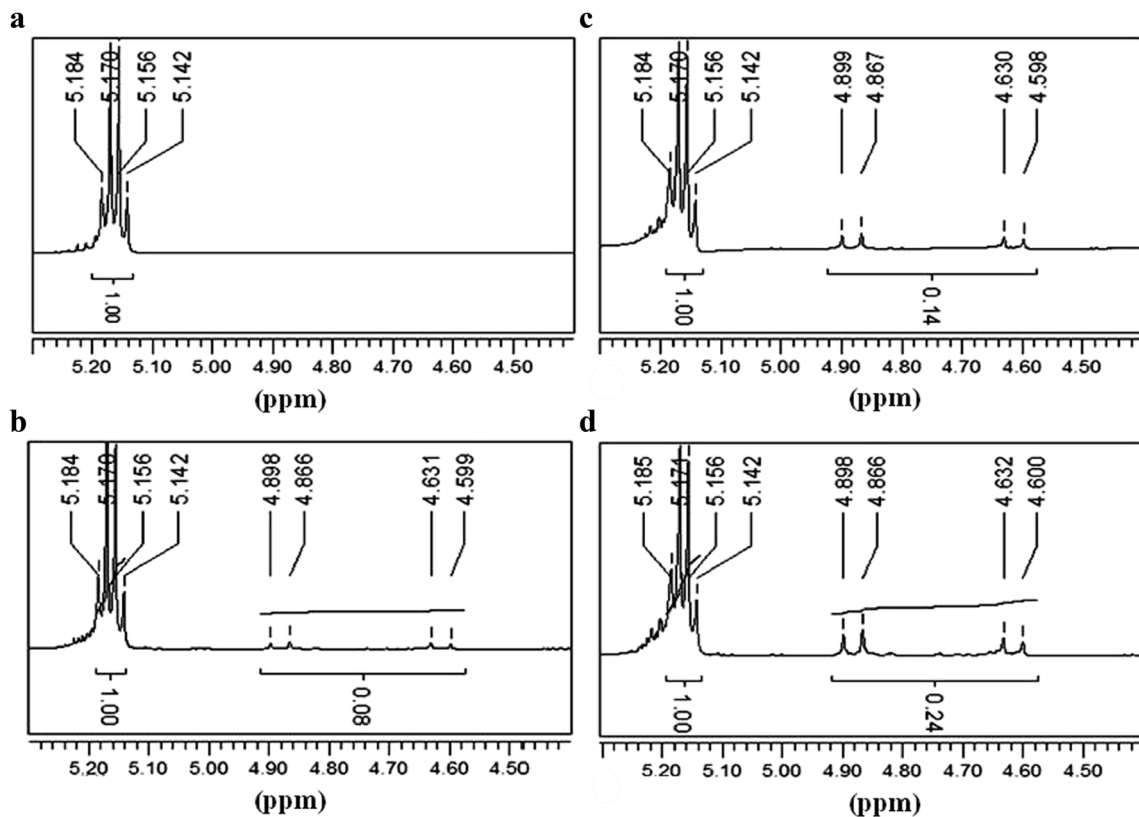
Fig. 8 ^{1}H NMR spectrum (500 MHz) of the copolymers as a function of the GA content (methine region for LA and methylene region for GA): **a** 0 mol%, **b** 2.5 mol%, **c** 5 mol%, and **d** 7.5 mol%
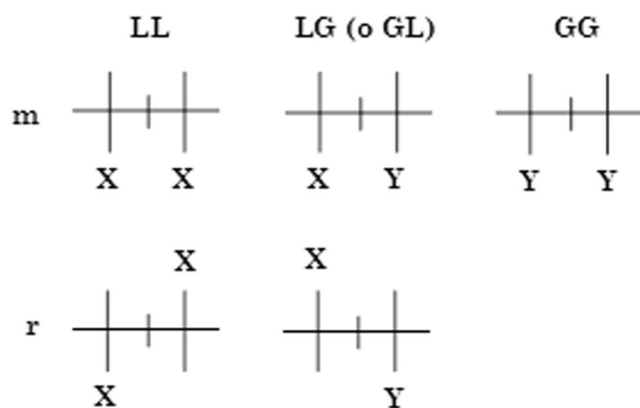
Fig. 9 Sequential configuration of dyads in the copolymers (m = meso; r = racemic). X = methyl of the C^2 corresponding of the lactic acid monomer units; Y = Proton of the C$^{2'}$ corresponding of the glycolic acid monomer units

Table 4 Sequence of average lengths of the copolymers from ^{13}C NMR

Samples Mole %	L_L	L_G
100.0/0.0	-	-
97.5/2.5	13.91	1.06
95.0/5.0	10.09	1.30
92.5/7.5	6.54	1.35

methine in LA and methylene in GA. The methine protons in LA generate a quadruplet signal between 5.1–5.3 ppm, and the methylene protons in GA result in a doublet of doublets between 4.6–4.9 ppm, which become more intense with the GA content.

^{13}C high resolution nuclear magnetic resonance (NMR) studies allowed for the determination of the type of resulting copolymers. This determination was based on the measurement of the chemical shifts observed in the ^{13}C spectra, and these shifts were affected by the adjacent atoms. The determination was made through measurement of the signal intensity and concentration integrations based on the distribution of dyads, which describe the arrangement of the monomers along the chain [20]. The combination of sequences is shown in Fig. 9, where L represents lactic acid and G represents glycolic acid. The number of sequences increases due to the chirality of the lactic acid monomer

approximately 11 % for the 2.5 GA sample, therefore, this contribution to melting should be considered in the results.
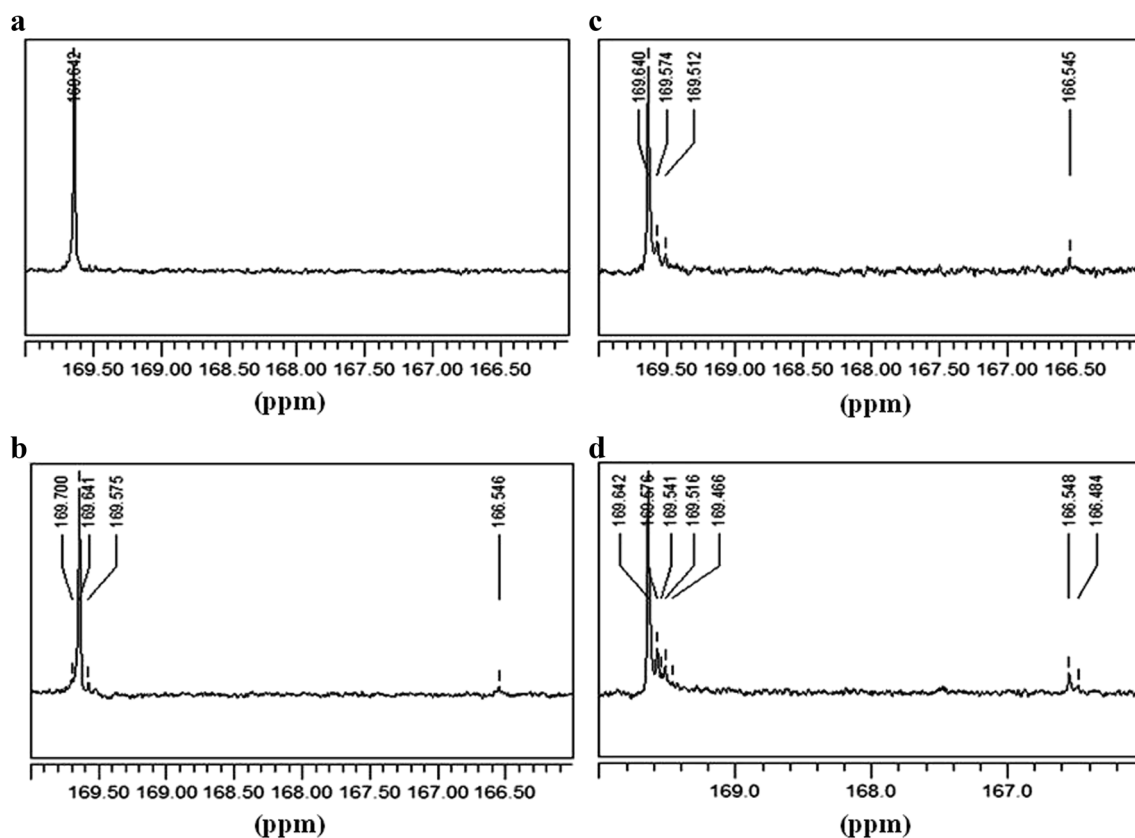
Figure 8 shows the ^{1}H NMR spectra as a function of the composition, where chemical shifts associated with the proton nuclei in the copolymers were observed. Overall, the spectra imply that the proton signals from nuclei are affected by the composition, which results in complex couplings that intensify with the content of glycolic acid. The spectra show the typical range for the proton chemical shift corresponding to

Fig. 10 ^{13}C NMR spectrum (500 MHz) of copolymers as a function of the GA content (carbonyl region): a 0 mol%, b 2.5 mol%, c 5 mol%, and d 7.5 mol%

The ^{13}C spectra were used for configuration analysis because the signal corresponding to the carbonyl group is the most appropriate due to its sensitivity to methyl, methylene and methine groups [18]. The ^{13}C spectra of the samples in the carbonyl group region are shown in Fig. 10. Here, an isolated peak was observed for lactic acid (Fig. 10a). However, with the addition of glycolic acid, the formation of new peaks at 166.55 and 166.50 ppm was observed. These new peaks become more intense as the glycolic acid content rises during polymerization (see Figs. 10 (b)-(d)). Therefore, the previous signals must correspond to linked glycolic and lactic acid (GL) and glycolic glycolic acid (GG), respectively [2].

Additional signals that are close to the main peak of the lactic acid carbonyl group (169.64 ppm) appeared and are intensified with the molar ratio of glycolic acid. These are however due to racemic sequential configurations in the copolymer. The average block length of lactic acid (L_L) and glycolic acid (L_G) was calculated from the integration of the signals using [18]:

$$L_L = \frac{I_{LL} + I_{LG}}{I_{LG}} \rightarrow \text{and} \rightarrow L_G = \frac{I_{GG} + I_{GL}}{I_{GL}} \quad (4)$$

where I_{LL} is the integral linked to the lactic acid unit and I_{LG} is the integral assigned to the unit of lactic acid linked to glycolic acid. I_{GG} is the integral of the signal assigned to the glycolic acid units that were linked together, and I_{GL} is the integral of glycolic acid units linked to lactic acid units.

Table 4 shows the average block length of the sequences in the synthesized P(L-LA/GA) copolymers. The average lengths of the lactic acid (L_L) chains decreased with the concentration of glycolic acid and the average lengths of glycolic acid (L_G) only suffered a small change. Therefore, we conclude that, with the continuous disproportions between both block lengths, the resulting copolymer product gradually gets a higher amount of GA repeat units into the main chain.

Chemical analysis

FT-IR spectroscopy was used to monitor the formation of the P(L-LA/GA) copolymers during polycondensation by azeotropic distillation. The corresponding spectra and reference standard, which were isothermally crystallized at 105 °C for 30 min, are shown in Fig. 11. In order to correct for film thickness the results were normalized respect to the C-O
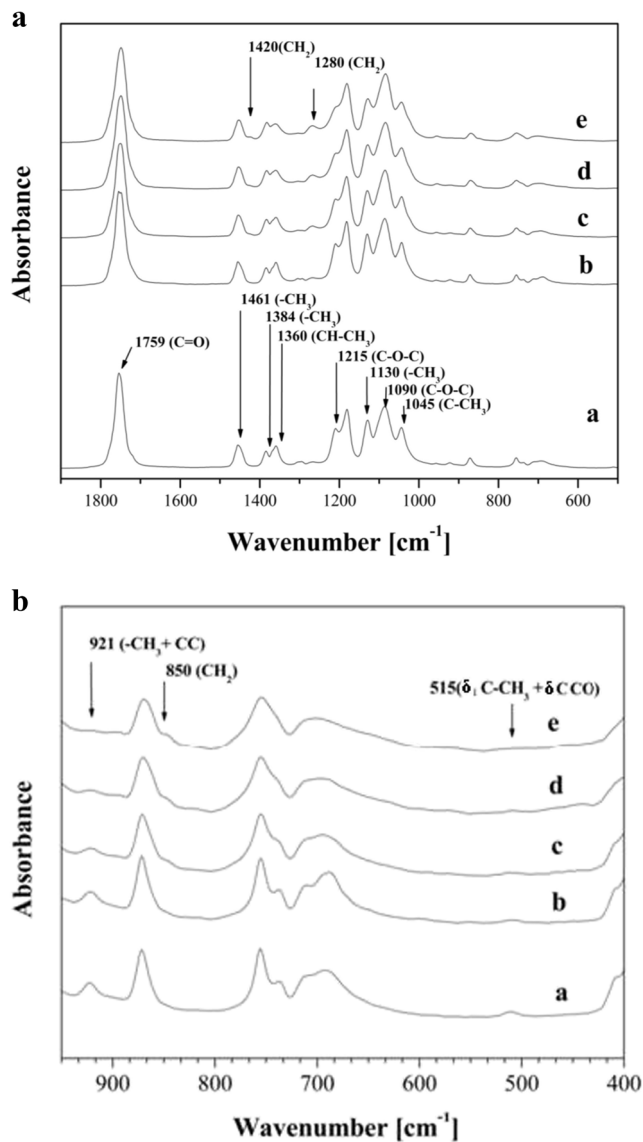
Fig. 11 **a** FTIR spectra of: a) P(L-LA) Std., b) 0 mol%, c) 2.5 mol%, d) 5 mol% and e) 7.5 mol% glycolic acid after isothermal crystallization (Tc = 105 °C; *t* = 30 min); **b** amplified FTIR spectra of: a) P(L-LA) Std., b) 0 mol%, c) 2.5 mol%, d) 5 mol% and e) 7.5 mol% glycolic acid after isothermal crystallization (Tc = 105 °C; t = 30 min)
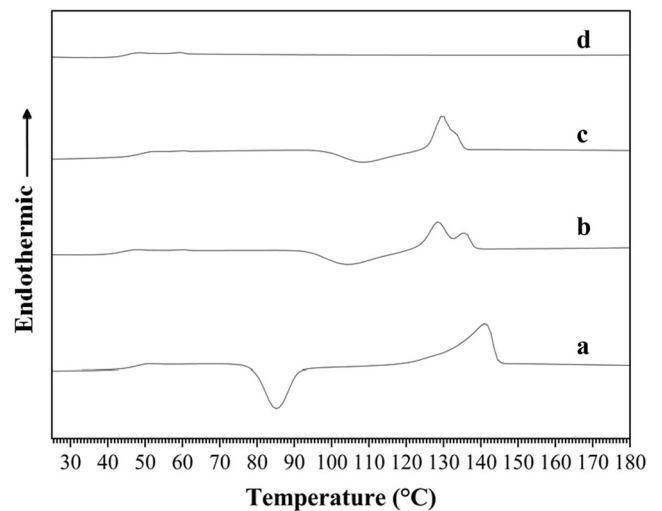
Fig. 12 DSC heating traces from the amorphous state of P(L-LA/GA) copolymers: **a** 0 mole %, **b** 2.5 mole %, **c** 5 mole % and **d** 7.5 mole % of glycolic acid
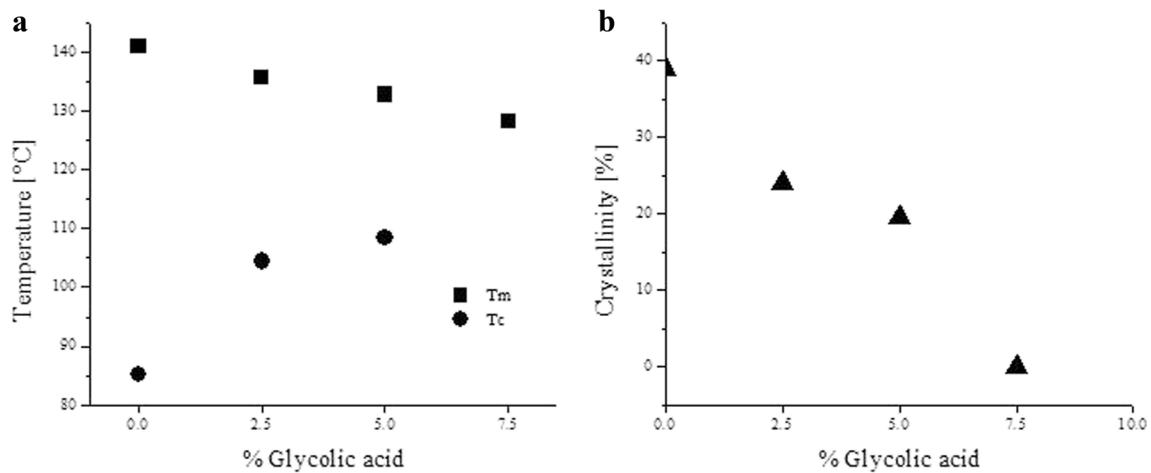
Fig. 13 Effect of the glycolic acid composition (mole %): **a** characteristic temperatures T_m and T_C and **b** crystallinity %

vibration band which is present in all products and it is approximately constant independently of their nature.

The FT-IR spectra of P(L-LA) exhibited characteristic peaks of particular vibrations or of the polymer functional groups. For example, the strong peak at 1759 cm^{-1} in Fig. 11(a) corresponds to stretching of the C = O group, at 1461 cm^{-1}, a less intense peak corresponds to CH$_3$, and two additional peaks at 1384 and 1360 cm^{-1} match the asymmetric deformation of CH. On the other hand, Zhang et al. (2005) reported that the band at ~1215 cm^{-1} corresponds to the C-O-C vibration and the

structural order of the CH$_3$ group in the crystalline phase [11, 21–24]. In addition, in Fig. 11(b), there is a band at 921 cm^{-1} which has been assigned to the combination of two vibrations (−CH$_3$ + CC) and represents the coupling of the CC backbone stretching with the CH$_3$ rocking mode [7, 22]. It is sensitive to the 10/3 helix chain conformation of the PLLA α or α′ crystal [21, 25]. An additional band that also corresponds to the semicrystalline state is present a 515 cm^{-1} and it was labeled according to the original source as (δ$_1$C-CH$_3$ + δCCO) [11]. This last vibration was reported as a weak (w) FTIR or medium (M) Raman band that corresponds to the semicrystalline (α, α′) state. It represents the coupling of bending of the CH$_3$ group [26] and the skeletal CCO bending [27].

In Fig. 11, there are vibrations that do not correspond to the semicrystalline state, such as those assigned to the group CH$_2$. The band at 850 cm^{-1} represents the CH$_2$ rocking mode, the one at 1280 cm^{-1} the CH$_2$ twisting and that at 1420 cm^{-1} the CH$_2$ bending vibration of the glycolic acid [28]. As indicated before, the group of bands at ~1215, 921 and 515 cm^{-1} are all related to the semicrystalline state, therefore, a decrease in the intensity of this group is a first indication that as the GA
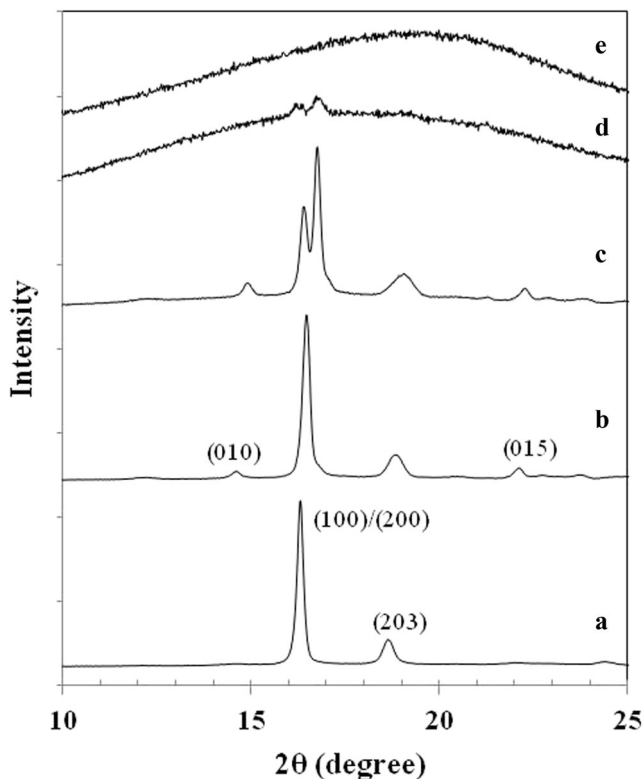
Fig. 14 WAXD patterns of: **a** Std. PLA, **b** 0 mol%, **c** 2.5 mol%, **d** 5 mol% and **e** 7.5 mol% of glycolic acid after isothermal crystallization (Tc = 105 °C; t = 30 min)
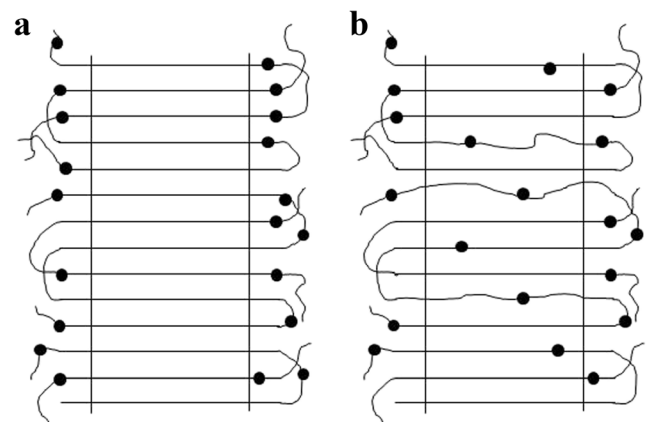
Fig. 15 Schematic representation of the two extreme models for lamellar crystalline random copolymers: **a** exclusion and **b** inclusion [17, 32]
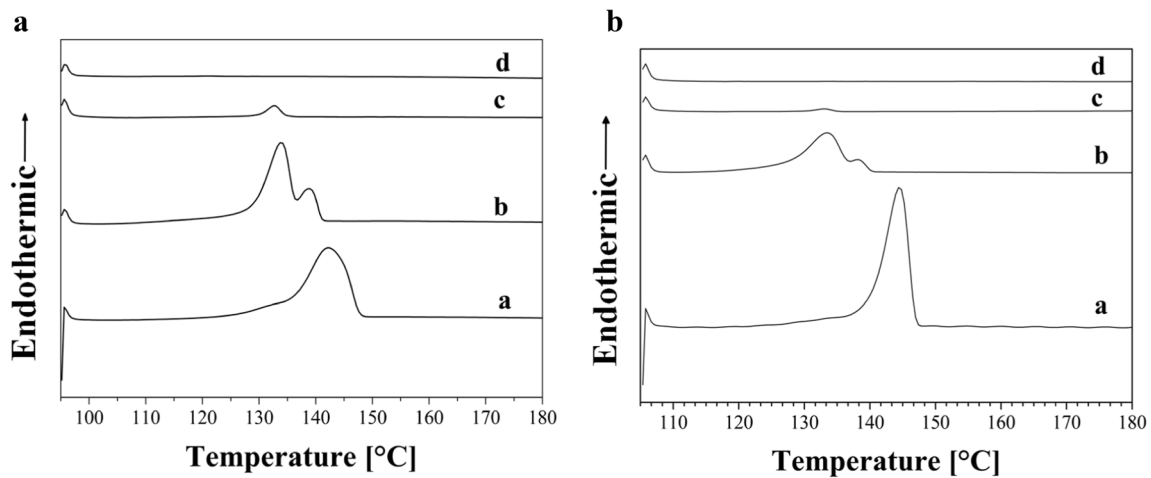
Fig. 16 DSC heating traces after isothermal crystallization from the melt of P(L-LA) homopolymers and P(L-LA/GA) copolymers: **a** (Tc = 95 °C; 30 min); **b** (Tc = 105 °C: 30 min); a) 0 mol%, b) 2.5 mol%, c) 5 mol% and d) 7.5 mol% glycolic acid

content increases the copolymer tends to an amorphous system, as will be demonstrated later with the DSC results.

Thermal properties

Figure 12 shows the heating traces from the amorphous state of the copolymers with various molar ratios of glycolic acid using $SnCl_2.2H_2O/TSA$ as the catalyst and a reaction time of 48 h. For the P(L-LA) reference, an exothermic crystallization peak was observed at 85 °C along with a melting endotherm at 141 °C. For the copolymers, an increase in the content of glycolic acid leads to a complex change in the melting behavior, which passes through a double melting endotherm and ultimately reaches an amorphous state. This behavior is similar to that reported for other engineering exclusion copolymers, such as poly (ethylene terephthalate)-co-poly (1,4 cyclohexylene dimethylene terephthalate) (PET/CT) [29]. The results also indicate that the amorphous state of these copolymers is reached when the ratio of glycolic acid exceeds 5.0 mol%. In copolymer systems, there

are two possibilities for crystallization. First, one of the copolymers can be included in the main crystals (inclusion copolymers). Second, a component is molecularly excluded from the main crystal (exclusion copolymers). In exclusion copolymers, a low concentration copolymer is rejected from the main crystal and forms its own low melting secondary crystals as long as the rejected molecular segments are also able to crystallize [29]. This behavior was observed for the exclusion P(ET/CT) system at low concentrations of CT [29] and now in the P(L-LA/GA) copolymer studied here.

The melting and crystallization temperatures of the copolymers together with the crystallinity as a function of glycolic acid mole fraction in the reaction mixture are shown in Fig. 13. A typical relationship of exclusion copolymers is observed between crystallization and melting temperatures in Fig. 13 (a), as the GA concentration augmented, the crystallization and melting temperatures converged. Figure 13(b) also shows the concentration at which the system loses its ability to crystallize due to the P(GA) concentration. The lack

Fig. 17 POM melting micrographs of P(L-LA), after isothermal crystallization at 105 °C (30 min). **a** 105 °C, **b** 125 °C, **c** 135 °C, **d** 140 °C, **e** 145 °C and **f** 146 °C
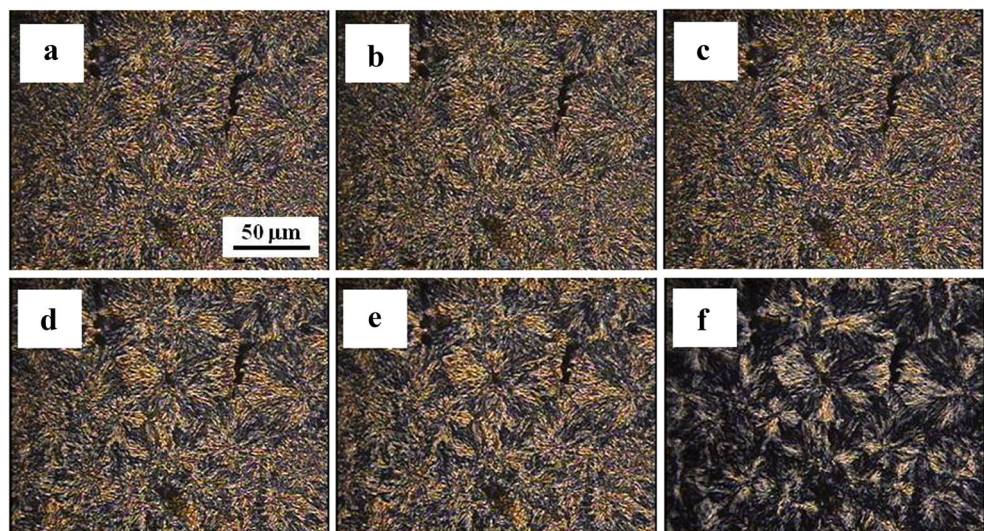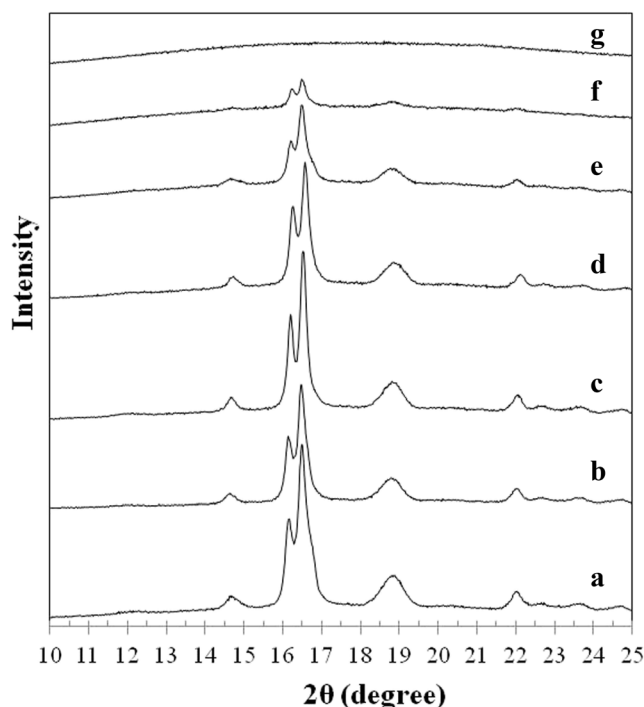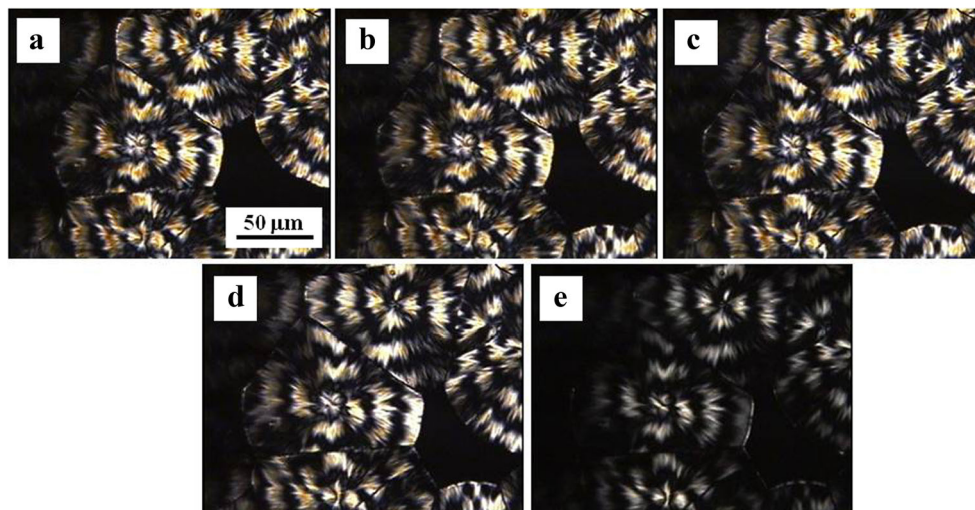
of crystallization at a given concentration is a feature of exclusion copolymers when the crystallizable sequences are equivalent to the non-crystallizable sequences, resulting in an amorphous system [20].

Crystallization

The complex crystal evolution was determined by WAXD as a function of the glycolic acid composition. For samples crystallized at 105 °C for 30 min, the results are shown in Fig. 14. Here, two diffracting peaks at 2θ = 16.4° and 18.6° were observed for the PLA standard, which are the characteristic diffracting planes of the unstable α' crystal structure [7, 22, 30]. The reference PLA, Fig. 14(b), generated the formation of other families of crystal planes, (010) and (015) at 2θ = 14.5° and 22° respectively. This complete set of crystal planes is associated to the more stable α crystal structure [31]. In a third change (Fig. 14(c), the formation of a new family of crystal planes at 2θ = 16.2° specifically corresponds to the α" crystal form [31]. This last is considered to have poor chain packing and lower crystal density compared to α and α′ crystal structures. In other studies [7, 30], the crystallization of P(L-LA) between 100 and 120 °C led to changes between the α' and α structures. In contrast, in the present work the increase in the content of glycolic acid induced a blended α-α" structure, as shown in Fig. 14 and in agreement with recent reports by Huihui Y. et al. [5].

As previously mentioned copolymers of two components A and B can crystallize in two forms. In the first case (Fig. 15a), the unit A crystallizes with a total rejection of the B units, which results in the formation of a two-phase system [32, 33]. In other words, the crystalline phase is formed by A units in equilibrium with an amorphous phase that is primarily composed of B units. In the second case, for the inclusion regimen, Fig. 15(b), the units of A and B can crystallize into a unique crystal structure [17, 32, 33].

Fig. 19 WAXD patterns of P(L-LA/GA) 2.5 GA after isothermal crystallization at 105 °C (30 min): **a** 105 °C, **b** 125 °C, **c** 130 °C, **d** 133 °C, **e** 135 °C, **f** 137 °C y **g** 140 °C

The ^{13}C NMR results allowed infer that the copolymers gradually get a higher proportion of rejectable and crystallizable GA units in the main chain. Furthermore, the DSC results in Fig. 12 show that, during melting, there is a gradual enhancement of the first melting endotherm proportional to the increase in GA content. Therefore, such as in the P(ET/CT) copolymers [29], as a first option we correlate the first endotherm to melting of the excluded and secondarily crystallized GA units. Although in the present case the first melting endotherm (i.e. the amount of secondary crystallization) is more

Fig. 18 POM melting micrographs of P(L-LA/GA) 2.5 GA, after isothermal crystallization at 105 °C (30 min): **a** 105 °C, **b** 115 °C, **c** 125 °C, **d** 135 °C and **e** 140 °C

pronounced compared to that of the P(ET/CT) system [29]. Therefore, a complementary explanation is needed.

As proposed in our so called step-like crystallization and melting hypothesis for the behavior of P(ET/CT) copolymers [29], the rejected CT sequences emerge from the edges of primary crystals and have the ability to act as new heterogeneous nuclei, forming secondarily branched crystal structures. Under linear heating, the isothermal crystals step-like melt, in an opposite manner to their formation, although crystal perfection and crystal thickening are not discarded [34].

The melting behavior of P(L-LA) homopolymers and P(L-LA/GA) copolymers was also investigated at other crystallization temperatures, and the results are shown in Fig. 16 (a) and (b). The melting/exclusion effect and the formation of an amorphous system were preserved at other crystallization temperatures.

In order to test the step-like melting hypothesis in P(L-LA), POM micrographs after isothermal crystallization at 105 °C (30 min.) were taken. The last micrograph of the crystallization process is shown in Fig. 17a where the main features of the picture are the high nucleation density and the rather undefined crystal morphology. During the melting process (Fig. 17b-f), PLLA behaves just as high temperature polymers. Newton's series colors disappear (i.e those related to thick crystalline areas) at the first melting endotherm, giving account of a step of melting that involves secondary crystalline structures. However, such as in PEEK [35], the main change in coloration occurs 145 °C, temperature inside the unique melting endotherm, as observed in Fig. 16(b).

The crystallization and melting POM results for P(L-LA/GA) 2.5 mol% GA are shown in Fig. 18, where as a consequence of the exclusion effect, more drastic changes have occurred. There is a lower nucleation density and banded spherulites are present. Banded spherulites often occur by thermal effects [13, 36], here however it is shown that the rejection of molecular GA sequences leads to banded spherulites, often interpreted as twisting lamellae.

During the P(L-LA/GA) melting process (Fig. 18 b-e), secondary colors start to disappear earlier than in the P(L-LA) case, in particular the melting process starts at 125 °C. This temperature marks the beginning of the first melting endotherm in Fig. 16(b)b.

The WAXD patterns of Fig. 19 were taken during melting and some amount of crystal perfection is observed. Crystal perfection is one of the recrystallization mechanisms and occurs around 130 °C, temperature at which the crystal planes increase its intensity in approximately 11 %. Furthermore, and such as in PET, recrystallization to thicker structures also occurs, however, this contribution has not been considered significant before [29]. In the present work, using the small angle X-ray scattering technique (the complete results are not shown here) we determined approximately 6 % increase in long period up to 125 °C,

temperature where the scattering contrast drastically decreased. On the other hand, if one wants to assume the recrystallization hypothesis [37], the particular case in Fig. 16(b)b would be one where the expected recrystallization should be minimal since the second melting endotherm is very low. Therefore, the first melting endotherm in this work is the result of melting of secondary crystalline structures in high proportion, say 80 %, originated by rejected GA segments and the increase in molecular weight. Recrystallization by perfection and thickening are complementary effects in this endotherm.

Conclusions

Polymerization by azeotropic distillation is a suitable route for synthesizing P(L-LA) homopolymers. The optimum reaction conditions include moderate temperatures, high reaction times and $SnCl_2.2H_2O$/TSA as a catalyst, which yield the polymeric products with higher stereochemical order. These reaction conditions allowed for the determination of the molecular characteristics and morphological behavior of the P(L-LA/GA) copolymers as a function of the GA content. The P(L-LA/GA) copolymers were considered exclusion copolymers with a step-like crystallization and melting behavior similar to other engineering polymers and copolymers. The formation of secondary crystals was associated with the excluded GA fraction and both the primary and secondary crystals developed the α-α" blended crystal structure. After the analysis of experimental results, the first melting endotherm was considered a combination of melting of secondary crystals in high proportion and recrystallization effects in lower proportion.

References

1. Aou K, Kang S, Hsu SL (2005) Morphological study on thermal shrinkage and dimensional stability associated with oriented poly(lactic acid). Macromolecules 38(18):7730–7735

2. Lan P et al. (2004) Studies on the synthesis and thermal properties of copoly(l-lactic acid-glycolic acid) by direct melt polycondensation. J Appl Polym Sci 92(4):2163–2168

3. Makadia HK, Siegel SJ (2011) Poly lactic-co-glycolic acid (PLGA) as biodegradable controlled drug delivery carrier. Polymers (Basel) 3(3):1377–1397

4. Saeidlou S et al. (2012) Poly(lactic acid) crystallization. Prog Polym Sci 37(12):1657–1677

5. Yin H et al. (2015) Synthesis and structure control of L-lactic acid–glycolic acid copolymer by homocopolymerization. J Appl Polym Sci 132(9):41566(1–6). doi:10.1002/app.41566

6. Marras SI, Zuburtikudis I, Panayiotou C (2007) Nanostructure vs. microstructure: morphological and thermomechanical

characterization of poly(l-lactic acid)/layered silicate hybrids. Eur Polym J 43(6):2191–2206

7. Pan P, Inoue Y (2009) Polymorphism and isomorphism in biodegradable polyesters. Prog Polym Sci 34(7):605–640

8. Mano JF et al. (2004) Bioinert, biodegradable and injectable polymeric matrix composites for hard tissue replacement: state of the art and recent developments. Compos Sci Technol 64(6):789–817

9. Lu JM et al. (2009) Current advances in research and clinical applications of PLGA-based nanotechnology. Expert Rev Mol Diagn 9(4):325–341

10. Nam JY et al. (2006) Morphology and crystallization kinetics in a mixture of low-molecular weight aliphatic amide and polylactide. Polymer 47(4):1340–1347

11. Auras, R.A., et al., (2011) Poly-lactic acid. Synthesis, structures, properties, processing, and applications. 10:100–107. Wiley

12. Ajioka M et al. (1995) The basic properties of poly (lactic acid) produced by the direct condensation polymerization of lactic acid. J Environ Polym Degrad 3(4):225–234

13. Medellin-Rodriguez FJ et al. (1997) The triple melting behavior of poly (ethylene terephthalate): Molecular weight effects. J Polym Sci B Polym Phys 35(11):1757–1774

14. Chen H et al. (2011) Synthesis and characterization of side chain polymer with helical PLLA segments containing mesogenic end group. Polymer 52(2):400–408

15. Priftis D et al. (2009) Polymer grafted Janus multi-walled carbon nanotubes. Soft Matter 5(21):4272

16. Fakirov, S., (2008) Transreactions in condensation polymers. Wiley

17. Gan Z et al. (2001) Solid-state microstructures, thermal properties, and crystallization of biodegradable poly(butylene succinate) (PBS) and its copolyesters. Biomacromolecules 2(2):605–613

18. Erbetta CDAC et al. (2012) Synthesis and Characterization of Poly(D,L-Lactide-co-Glycolide) Copolymer. J Biomed Nanotechnol 03(02):208–225

19. Medellin-Rodriguez FJ et al. (2004) Melting behavior of polymorphics: molecular weight dependence and steplike mechanisms in nylon-6. Macromolecules 37(5):1799–1809

20. Gao Q et al. (2002) Direct synthesis with polycondensation and microstructure analysis of poly(l-lactic acidco-glycoluc acid). Polym J 34(11):786–793

21. Urayama H, Moon SI, Kimura Y (2003) Microstructure and thermal properties of Polylactides with different Land D-unit sequences: importance of the helical nature of the L-sequenced segments. Macromol Mater Eng 288(2):137–143

22. Zhang J et al. (2005) Crystal modifications and thermal behavior of poly(L-lactic acid) revealed by infrared spectroscopy. Macromolecules 38(19):8012–8021

23. Zhang J et al. (2004) Weak intermolecular interactions during the melt crystallization of poly(L-lactide) investigated by two-dimensional infrared correlation spectroscopy. J Phys Chem B 108(31): 11514–11520

24. Pan P et al. (2012) Temperature-variable FTIR and solid-State13C NMR investigations on crystalline structure and molecular dynamics of polymorphic poly(l-lactide) and poly(l-lactide)/poly(d-lactide) Stereocomplex. Macromolecules 45(1):189–197

25. Woo EM, Chang L (2011) Crystallization and morphology of stereocomplexes in nonequimolar mixtures of poly(l-lactic acid) with excess poly(d-lactic acid. Polymer 52(26):6080–6089

26. Aou K, Hsu SL (2006) Trichroic vibrational analysis on the α-form of poly (lactic acid) crystals using highly oriented fibers and spherulites. Macromolecules 39(9):3337–3344

27. Kang S et al. (2001) A spectroscopic analysis of poly (lactic acid) structure. Macromolecules 34(13):4542–4548

28. Kister G, Cassanas G, Vert M (1997) Morphology of poly (glycolic acid) by IR and Raman spectroscopies. Spectrochim Acta A Mol Biomol Spectrosc 53(9):1399–1403

29. Medellín-Rodríguez FJ et al. (1998) Triple melting behavior of poly (ethylene terephthalate co-1, 4-cyclohexylene dimethylene terephthalate) random copolyesters. J Polym Sci B 36(5):763–781

30. Pan P et al. (2007) Polymorphous crystallization and multiple melting behavior of poly(L-lactide) molecular weight dependence. Macromolecules 40(19):6898–6905

31. Marubayashi H et al. (2008) Crystalline structure and morphology of poly (L-lactide) formed under highpressure CO2. Macromolecules 41(23):9192–9203

32. Sanchez IC, Eby RK (1973) Crystallization of random copolymers. J Res Natl Bur Stand 77(3):353–358

33. Flory PJ (1955) Theory of crystallization in copolymers. Trans Faraday Soc 51:848–857

34. Avila-Orta CA et al. (2003) On the nature of multiple melting in poly (ethylene terephthalate)(PET) and its copolymers with cyclohexylene dimethylene terephthalate (PET/CT. Polymer 44(5):1527–1535

35. Medellin-Rodriguez FJ, Phillips PJ, Lin JS (1996) Melting behavior of high-temperature polymers. Macromolecules 29(23):7491–7501

36. Ramírez-Vargas E et al. (2000) Morphological and mechanical properties of polypropylene [PP]/poly (ethylene vinyl acetate)[EVA] blends. I Homopolymer PP/EVA systems. Polym Eng Sci 40(10):2241–2250

37. Roberts RC (1969) Poly (ethylene terephthalate) II—morphological changes on annealing. Polymer 10:117–125